Supporting Information

Early-stage deactivation of Pt-loaded TiO_2 using *in situ* photodeposition during photocatalytic hydrogen evolution

*Greta M. Haselmann, Dominik Eder**

Technische Universität Wien, Institut für Materialchemie, Getreidemarkt 9, 1060, Vienna, Austria.

*Email: dominik.eder@tuwien.ac.at

This document contains additional experimental data as well as calculations and complementary discussions of results.

S1. Calculation of quantum efficiencies

The quantum efficiency (QE) gives a measure for how well incident light can be converted into H_2. It is defined as the number of reacted electrons per incident photons and can be calculated from the measured activities during H_2 evolution experiments and the incident photon flux:

$$QE = \frac{\#\ of\ reacted\ electrons}{\#\ of\ incident\ photons}$$

For QE calculations, one could either use only the incident photons that can be theoretically absorbed by the material (e.g. $\lambda < 400$ nm for anatase TiO_2) or all incident photons (here: 280 – 500 nm). The first gives you a measure of how well your system itself can convert the photons it absorbs into chemical energy. The latter would provide a measure to compare different systems. This work considers all incident photons for QE calculations. It should be kept in mind, that scattering effects which are difficult to measure are usually neglected which

results in an overestimation of the amount of incident photons and a subsequent underestimation of the QE [1].

The overall incident photon flux for the UV mode was calculated from the theoretical incident photon flux supplied by the manufacturer and the ratio of the measured light power to the theoretical power (# of incident photons = 8.4×10^{21} photons h^{-1}). The number of reacted electrons could be calculated from the hydrogen evolved during a photoreforming experiment.

$$\#\ of\ reacted\ e^- = \frac{2\ mol\ e^-}{mol\ H_2}\ n_{H_2}\ N_A$$

Table S1 lists the maximum rates for H_2 evolution of the different Pt loadings discussed in the main text as well as their rates after deactivation if applicable and their corresponding QE.

Table S1. Overview on the photocatalytic activities and corresponding quantum efficiencies (QE) for all materials shown in this work correlated to their pretreatment using ultrasound (US) and (if applicable) the observed deactivation.

Pt loading	US? (Y/N)	Deactivation? (Y/N)	max. H_2 rate/after deactivation (µmol h^{-1})	max. H_2 rate/after deactivation (mmol h^{-1} g^{-1})	QE (λ = 280 - 500 nm)	QE (λ < 400 nm)
0.0 wt.%	N	N	8.8	0.17	0.13	0.26
0.0 wt.%	Y	N	2.8	0.056	0.04	0.08
0.25 wt.%	N	Y	739 / ~235	14.8 / ~4.7	11 / 3	22 / 7
0.25 wt.%	Y	Y	472 / ~210	9.4 / ~4.2	7 / 3	14 / 6
0.4 wt.%	N	N	1930	38.6	28	56
0.4 wt.%	Y	Y	1345 / ~235	26.9 / ~4.7	19 / 3	39 / 7
0.75 wt.%	N	N	2238	44.8	32	65
0.75 wt.%	Y	N	2128	42.6	30	62
1.0 wt.%	N	N	2127	42.6	30	62
1.0 wt.%	Y	N	2233	44.7	32	65
1.5 wt.%	N	N	2277	45.5	33	66
1.5 wt.%	Y	N	2196	43.9	31	64

S2. Additional experiments to investigate the impact of ultrasound

Extended ultrasound treatments

P25 was irradiated with ultrasound (US) for 1 min (black) and 30 min (red). Overall, the rate for hydrogen evolution was slightly lower after longer US irradiation. Still, the general shape and behavior are similar, so that 1 min was generally found to be sufficient for our purposes.

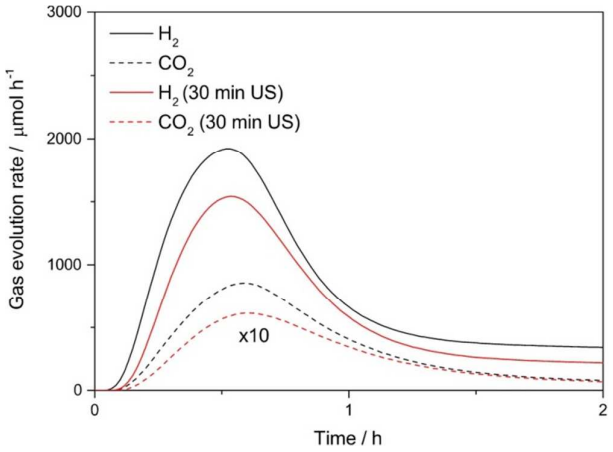

Fig. S1. Pt/P25 (0.5 wt.%) irradiated with ultrasound (US) before a photocatalytic experiment for 1 min (black) and 30 min (red). The point of deactivation did not shift, while the extent was slightly larger for the longer irradiation time.

Ultrasound irradiation of P25 in pure water and in aqueous methanol solution

P25 was generally irradiated with US in the 50 vol.% aqueous methanol solution. To see whether the methanol has a detrimental effect or might even be the cause for deactivation (*e.g.* due to incorporation of C), we also irradiated P25 in pure distilled water and added the methanol afterwards. Irradiation in absence of methanol led to a much less pronounced peak of the maximum rate. This could be caused by a considerably more pronounced deactivation of the Pt from the beginning of the experiment.

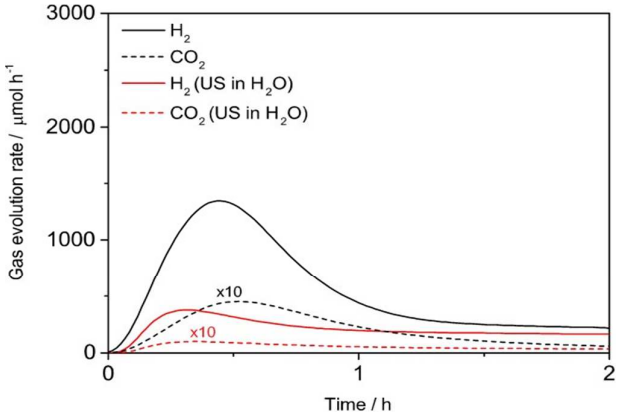

Fig. S2. Pt/P25 (0.4 wt.%) irradiated with ultrasound (US) before a photocatalytic experiment in 50 vol.% methanol (black) and pure water (red). Deactivation occurred earlier and overall performance was worse for the sample irradiated in absence of methanol.

S3. Additional materials characterizations and discussions

Overview of parameters extracted from various material characterizations

Table S2 gives an overview of the collected structural and morphological data using BET, powder XRD and DRS-UV-vis. Experimental conditions are listed to better correlate the findings to the photocatalytic behavior of the catalysts. Changes in the BET surface area were not found to be pronounced enough to account for the large difference in activities and were also not consistent with the deactivation behavior. The typical phase composition of P25 consisting of about 80% anatase and 20% rutile also did not change irregardless of US or UV irradiation. The band gap slightly decreased with an increasing amount of Pt as discussed in Section 5.7., but also not to an extent that could be accountable for the deactivation.

Table S2. Overview of BET measurements, band gap calculations from DRS-UV-vis, and phase composition from XRD patterns for the different Pt/P25 samples and their references.

Pt / wt.%	US / min	MeOH:H_2O / v:v	UV / h	Deactivation?	BET / $m^2 g^{-1}$	E_g / eV	I_R/I_A
0.0 (pristine P25)	---	---	---	---	55.3	3.18	0.18
0.0	30	0:1	---	---	53.2	2.99	0.18
	30	1:1	---	---	52.6	3.00	0.17
0.0	0	1:1	2	---	55.6	3.03	0.16
	1	1:1	2	---	45.8	3.03	0.18
0.25	0	1:1	2	Y	41.1	3.03	0.17
	1	1:1	2	Y	41.2	3.03	0.20
0.4	0	1:1	2	N	64.3	3.02	0.17
	1	1:1	2	Y	59.5	3.00	0.18
0.75	0	1:1	2	N	62.9	2.92	0.17
	1	1:1	2	N	60.2	2.98	0.18
1.0	0	1:1	2	N	61.9	2.94	0.18
	1	1:1	2	N	82.9	2.96	0.18
1.5	0	1:1	2	N	56.4	2.88	0.18
	1	1:1	2	N	60.1	2.91	0.19

Powder XRD patterns of Pt/P25

This is a systematic screening of all samples with and without US treatment for various Pt loadings.

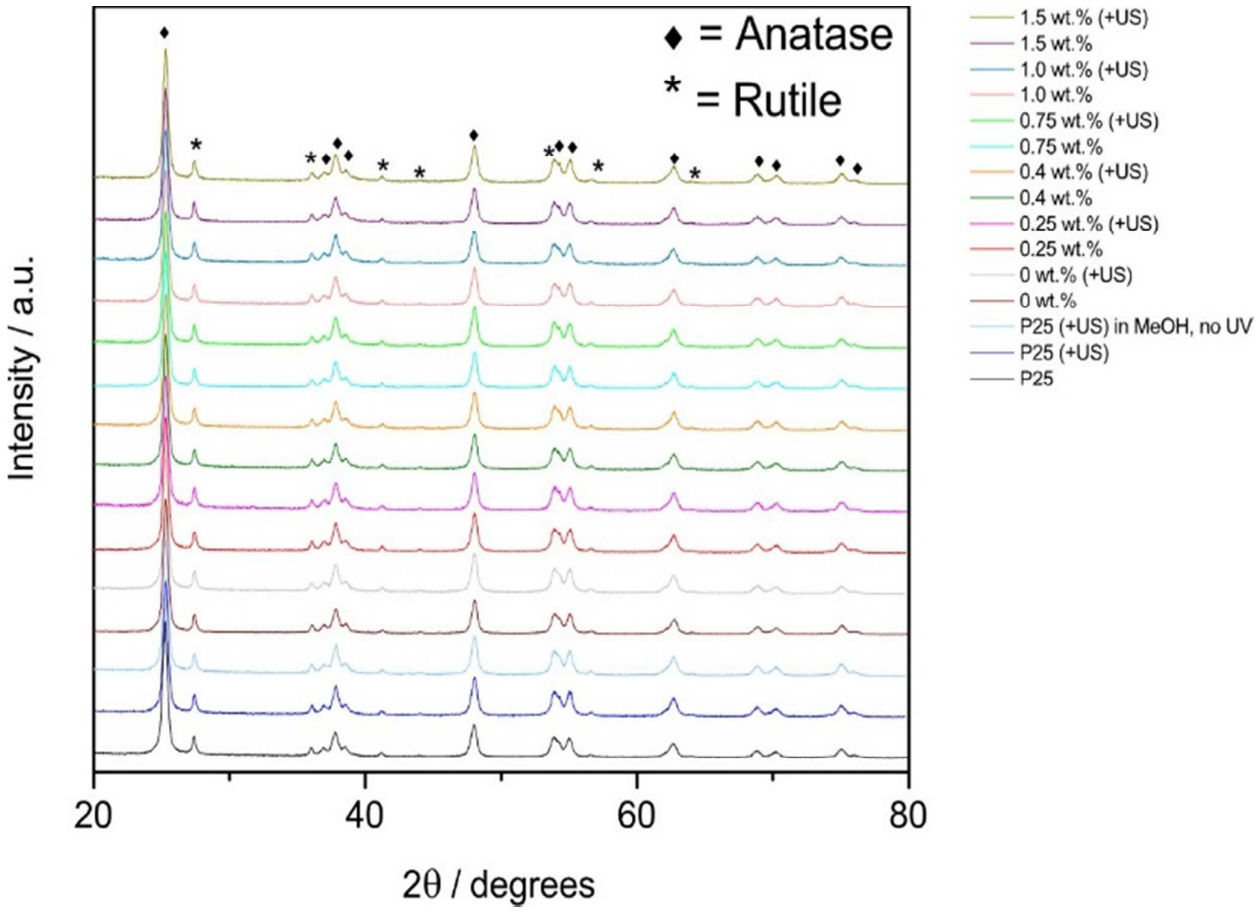

Fig. S3. Powder XRD patterns of Pt/P25, pristine P25 as well as P25 subjected to ultrasound in water and methanol solution for reference.

Additional HRTEM images

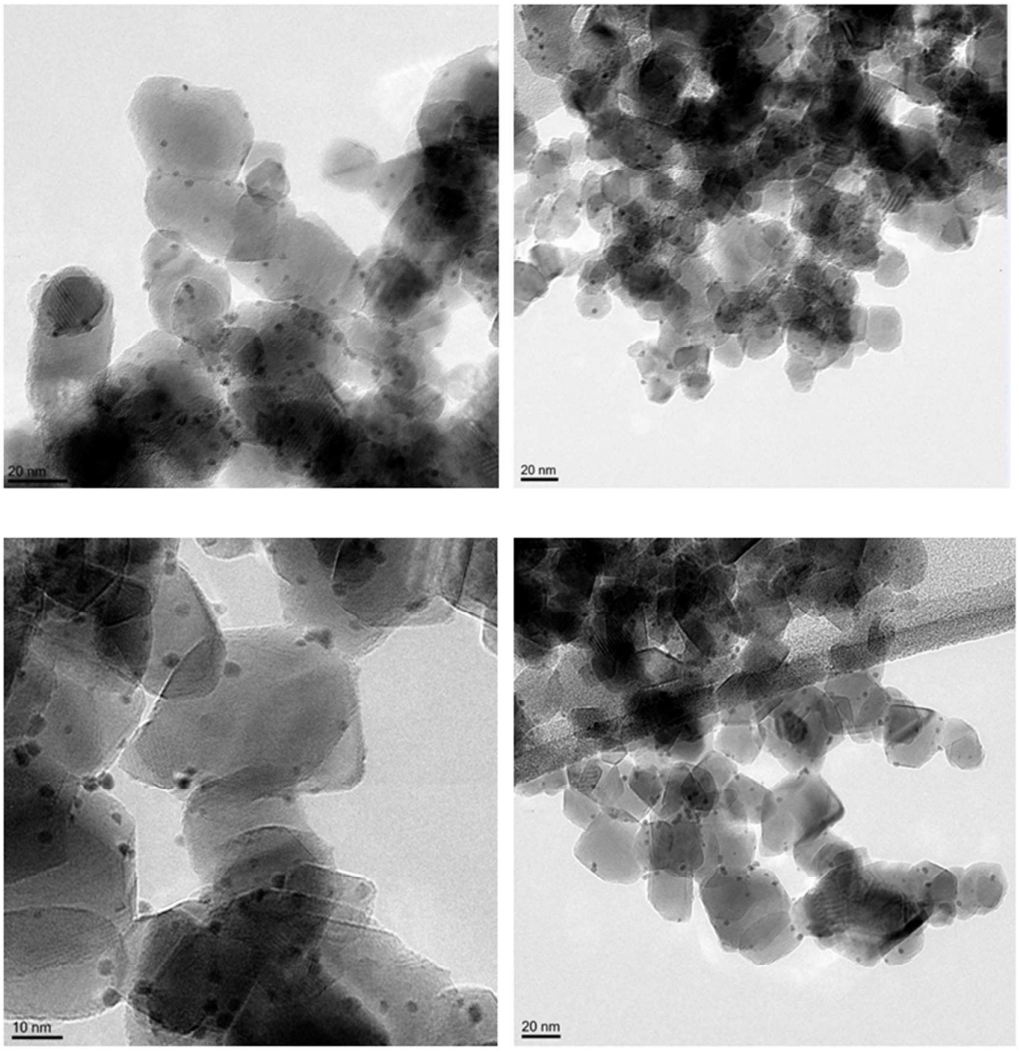

Figure S4. HRTEM images of non-ultrasonicated (top row) and ultrasonicated (bottom row) Pt-loaded P25.

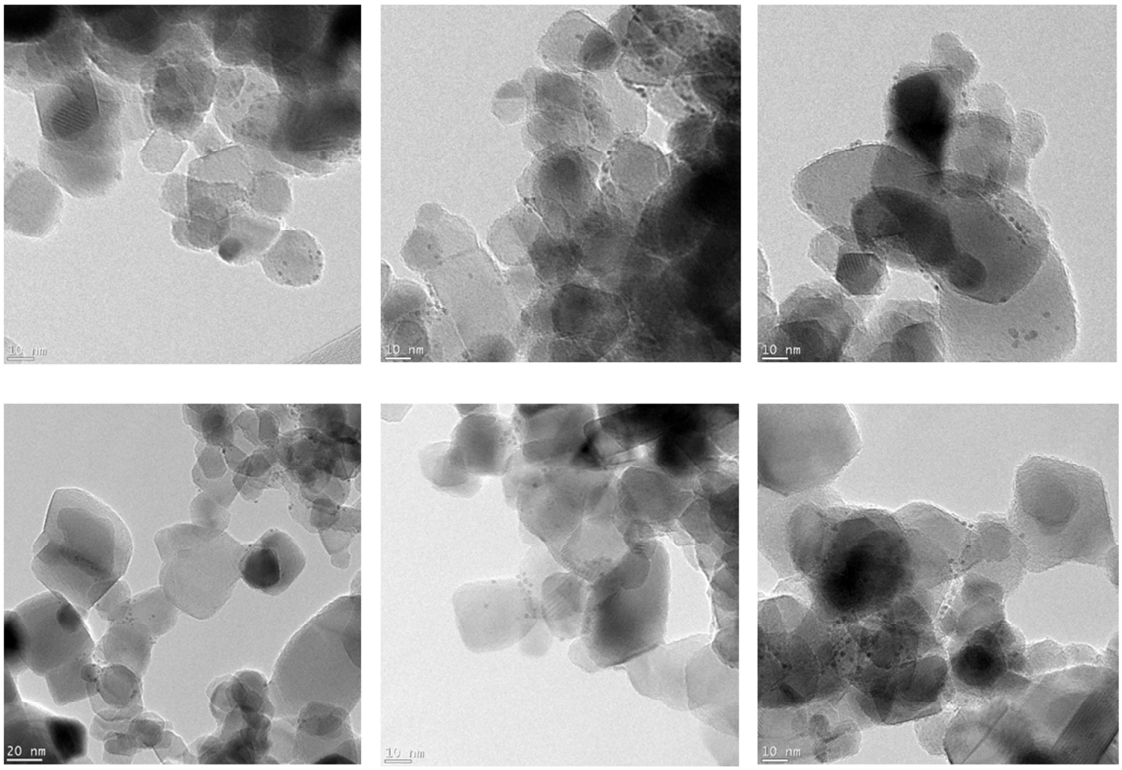

Figure S5. HRTEM images of non-calcined (top row) and calcined (bottom row) Pt-loaded P25.

We further considered the dispersion of Pt as a possible explanation, especially, as Ohtani et al. showed a dependence of the overall photocatalytic rate on the number of Pt-loaded TiO_2 nanoparticles rather than the total number of Pt deposits.[2] This explanation model would suggest that the deactivation could be caused by a gradual agglomeration of Pt that leaves more TiO_2 particles unoccupied and inactive. However, there were several arguments against this influence of dispersion: First of all, there were no obvious dispersion changes as observed with TEM. Additionally, the sudden deactivation after already 10 h of UV irradiation could not be explained by a gradual agglomeration of Pt particles. Also, this model would neither fit the dependency on methanol concentration, a repeated deactivation after re-using the photocatalyst nor the fact that a higher amount of vacancies (i.e. after US treatment) at the same Pt loading (0.4 wt.%) triggers deactivation. Lastly, the obvious correlation to the CO generation would not be well-explained by this model.

Absorption spectra of UV and US irradiated samples

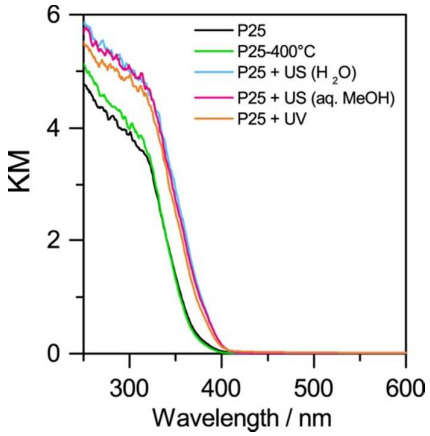

Figure S6. Absorbance spectra (in Kubelka-Munk) of pristine P25 (black), P25 treated at 400 °C in air for 5 h (green), P25 irradiated in destilled water (blue) and aqueous methanol solution (magenta), and P25 illuminated with UV light (orange).

Particle size distributions (PSD) of Pt particles on P25

PSD of Pt particles on P25 were obtained from statistical analysis of HRTEM images for all loadings (0.25 - 1.5 wt.%). At least 100 Pt particles for each loading were measured manually using ImageJ software to obtain a representative value for the size distribution. OriginPro 2015 software was used for statistical analysis. The median value of the Pt particle size did show a slight increase at loadings above 1.0 wt.%. However, a change in deactivation behavior is already observed below 0.75 wt.%, leading us to the conclusion that the particle size in our Pt loading range is not the critical factor for the observed drop in activity.

Table S3. Data from the particle size distribution for different Pt loadings on P25.

Pt / wt.%	US / min	Deactivated?	Total number of counted particles	Median / nm
0.25	0	Y	110	3.03
	1	Y	218	3.46
0.4	0	N	172	3.08
	1	Y	150	3.05
0.75	0	N	187	3.06
	1	N	103	3.13
1.0	0	N	332	3.76
	1	N	290	3.53
1.5	0	N	457	4.35
	1	N	304	3.89

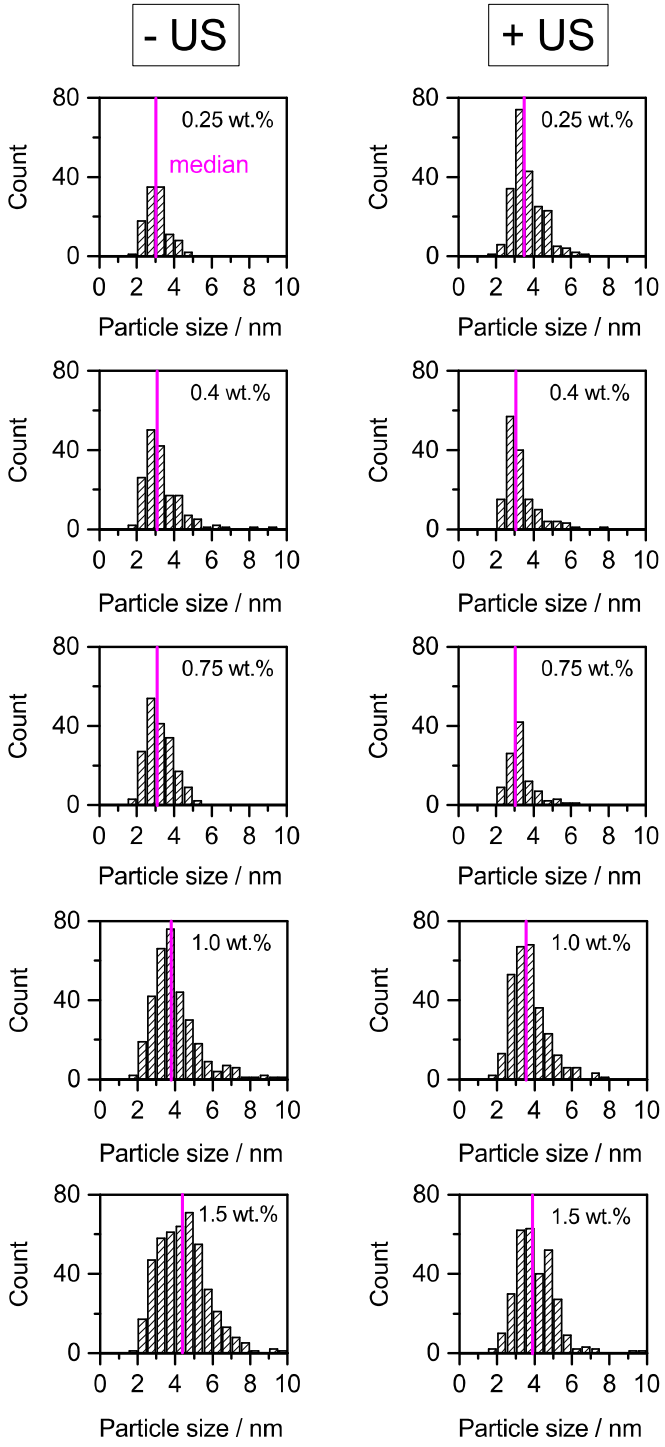

Fig. S7. Pt particle size distribution for Pt/P25 (0.25, 0.4, 0.75, 1.0, 1.5 wt.%) without and with pretreatment with ultrasound (- and +US, respectively).

DRS-UV-vis of Pt/P25

The DRS-UV-vis spectra of recovered P25 with all different Pt loadings are shown in Fig. S8. The corresponding Tauc plots are shown in Figure S9 and S10. Absorption in the visible range increases due to the Pt as described elsewhere [3]. Absorption below 400 nm and thus the band gap also increases slightly, which might be due to defects stabilized by Pt as described in the main text.

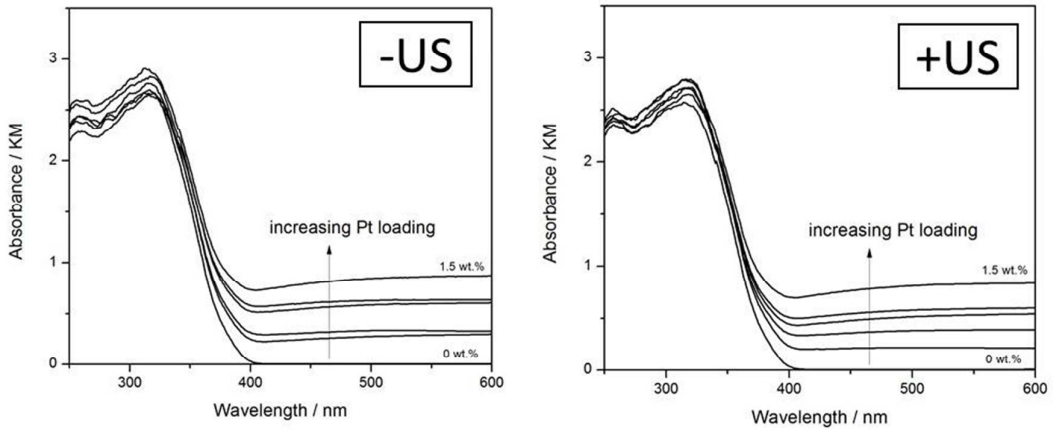

Fig. S8. DRS-UV-vis spectra in Kubelka-Munk units of Pt/P25 at different loadings with and without US pretreatment (+ US and –US, respectively).

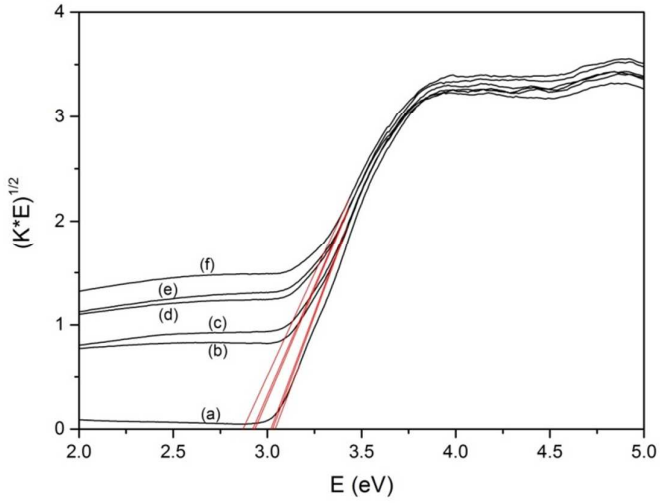

Fig. S9. DRS-UV-vis spectra of Pt/P25 for a loading of (a) 0.0, (b) 0.25, (c) 0.4, (d) 1.0, (e) 0.75, and (f) 1.5 wt.% Pt without a US pretreatment.

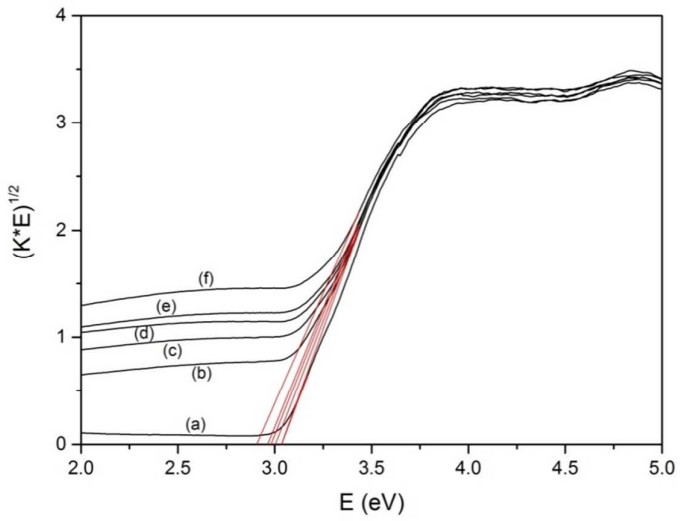

Fig. S10. DRS-UV-vis spectra of Pt/P25 for a loading of (a) 0.0, (b) 0.25, (c) 0.4, (d) 0.75, (e) 1.0, and (f) 1.5 wt.% Pt with US pretreatment.

HRTEM images of deactivated and not deactivated Pt-TiO_2

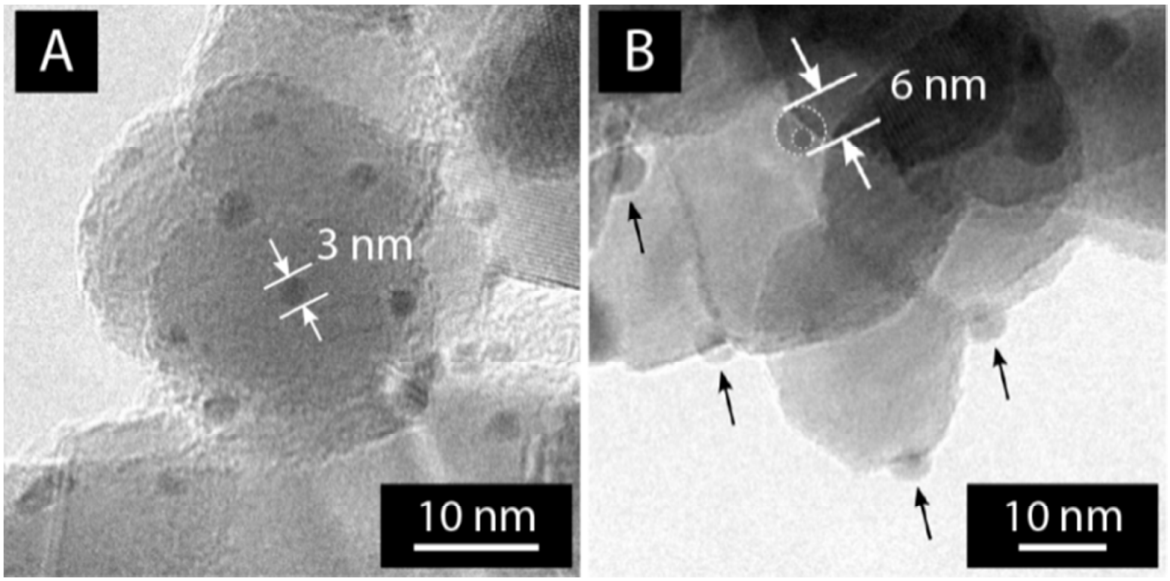

Fig. S11. HRTEM images of (A) not deactivated and (B) deactivated Pt/P25 recovered after photocatalytic experiments. The not deactivated sample shows typical dispersion of Pt particles (about 3 nm in size) on TiO_2 crystals, while Pt particles of the deactivated sample are encapsulated by a layer of about 1-2 nm of framework material.

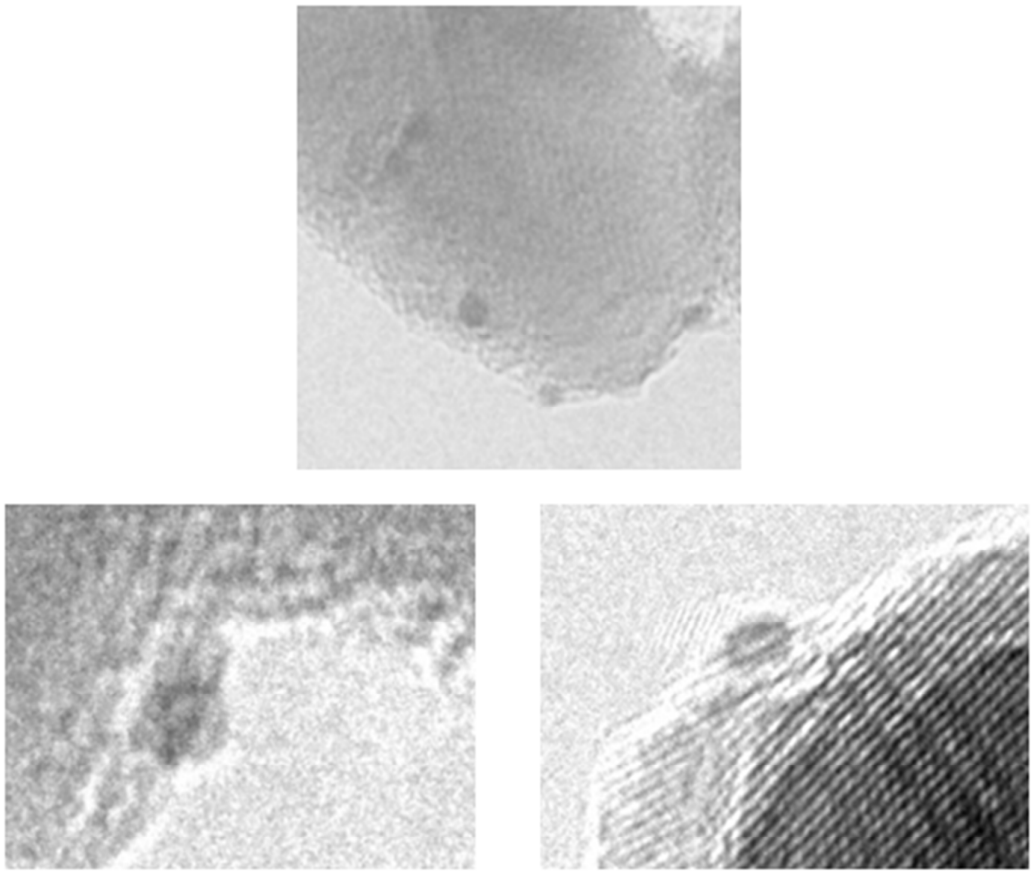

Fig. S12. HRTEM close ups of not deactivated sample.

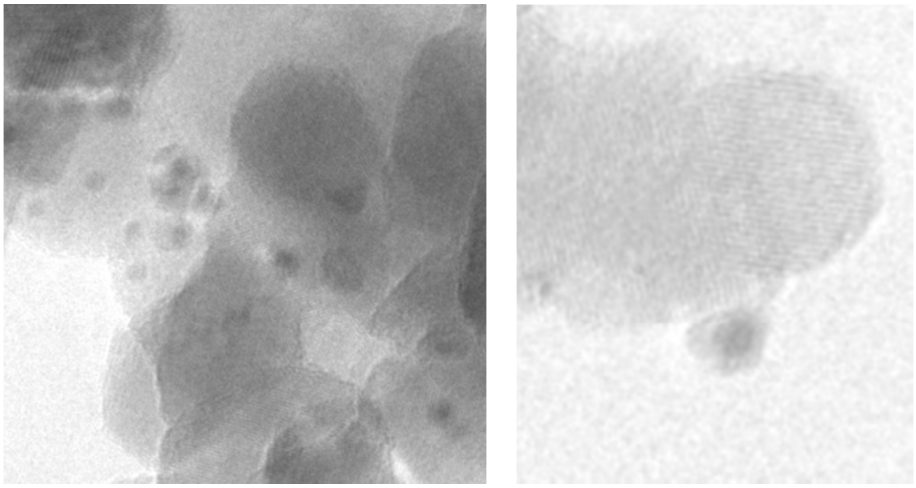

Fig. S13. HRTEM close ups of deactivated sample.

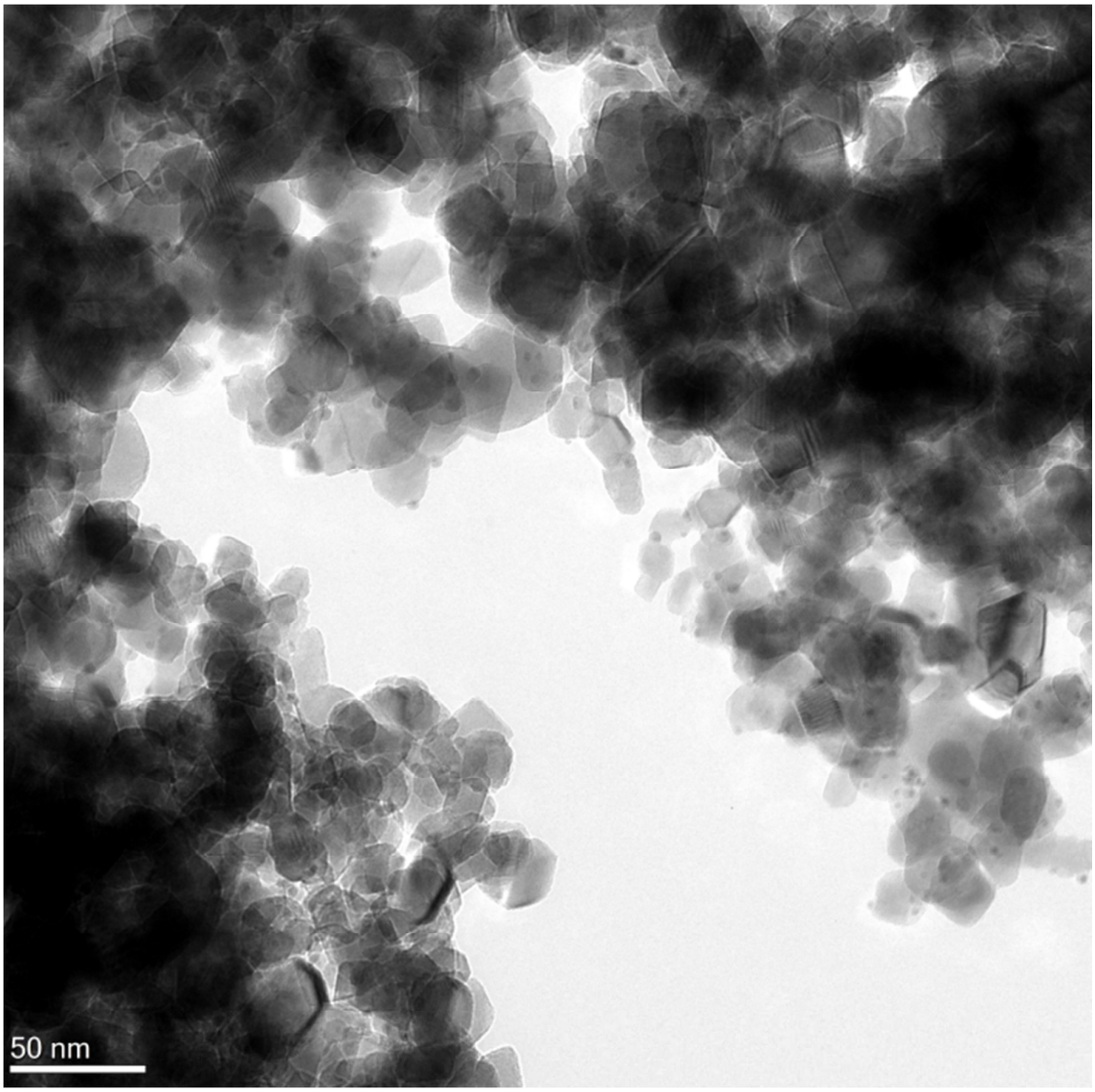

Fig. S14. HRTEM image of the deactivated sample.

REFERENCES:

(1) Kudo, A.; Miseki, Y., *Chem. Soc. Rev.* **2009**, 38, 253-278.

(2) Ohtani, B.; Iwai, K.; Nishimoto, S.-i.; Sato, S., *J. Phys. Chem. B* **1997**, 101, 3349-3359.

(3) Vijayan, B. K.; Dimitrijevic, N. M.; Wu, J.; Gray, K. A., *J. Phys. Chem. C* **2010**, 114, 21262-21269.